Numerical and analytical discussions of fracture propagation through soil in reverse faulting.

東京大学大学院　学生正会員　Sven P. Teodori
東京大学大学院　正会員　小長井　一男
東京大学大学院　正会員　Jorgen A.T. Johansson

1. Introduction. In the central part of Taiwan, an earthquake with a local magnitude of 7.3 (moment magnitude 7.6) occurred on September 21, 1999. Damages to very important structures occurred due to permanent soil deformations. Particularly, the Freeway route n^3, crossing several times the Chelungpu reverse fault, had several pier foundations, which were still under construction, damaged at Bauweishan, south of Nantou city. The bridge piers pile caps rotated, tilted, and translated due to the faulting induced soil deformations. Measurements of the pile-cap positions before and after the earthquake, pile coring, drilling, and SPT testing have permitted to estimate the underground soil strata geometry, the geomechanical properties, the possible location, the mechanism of the reverse fault, and the interaction with the structures. These data are very important for possible improvements to current building codes. Available field data are very important for obtaining input parameters for numerical simulations. The first step of this study is to understand how the soil's governing parameters influence its behavior in the case of reverse faulting; a simple model based on FEM and a mechanical analytical model are built-up and their solutions compared.

2. Numerical Modeling. Using a FEM model for understanding the phenomenon of reverse faulting, the objective is to find out which and how the input parameters influence the soil behavior, which are the important output parameters for engineering design.

A static 2D plane strain model with an elasto-plastic soil with a Mohr-Coulomb yield criterion was used. Neither inertial nor wave propagation effects were considered.

The observed different underground soil rigidity has been modeled as two distinct soil types: the sand-gravel as "hard soil" and the silt-clay as "soft soil", Fig.1.

The geometric parameters (Tab. 1) for defining this model are: the dip angle (α) of the separating material boundary fault line, the depth of the soil deposit (H), and lengths (Li), which were chosen as to avoid boundary effects.

The mechanical parameters (Tab. 2) necessary to define the model are for the soft soil: the Young's modulus (E) the Poisson's coefficient (ν), the friction angle (ϕ_S) and the cohesion (c) for the Mohr-Coulomb assumed rupture criterion, the dilatancy (ψ) as non-elastic property. The density (ρ) is necessary to implement the gravity (g). The fault line is modeled with a friction angle (ϕ_F). The hard soil is considered rigid. After a gravitational acceleration has been applied to the model, the boundary conditions (bottom and right one) displace (Δ_F) parallel to the fault line. The mesh consists mostly in 1m x 1m 8-node bi-quadratic plane strain quadrilateral and 6-node quadratic plane strain triangle element types.

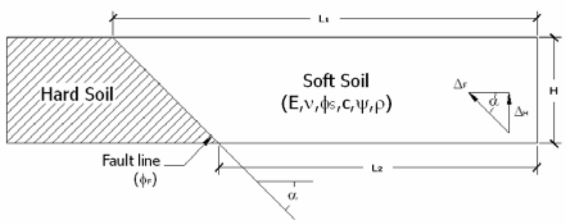

Fig.1 FEM model of 2D reverse faulting with two types of soils.

L_1 (m)	L_2 (m)	H (m)	α (°)	Δ_F (m)
160	120	40	45	0.5

Table 1 Geometry of the FEM model.

Fault line	Soft Soil					
ϕ_F (°)	E (MPa)	ν (–)	ϕ_s (°)	c (kPa)	ψ (°)	ρ (kN/m³)
30	100	0.3	35	1	6	16

Table 2 Mechanical properties of the FEM model.

3. Numerical outputs and solution. The most important numerical outputs to take into account in this study are the plastic strain distribution in the soil after the bedrock displacement has occurred, Fig.2. Even if the mechanical properties of the fault line seam to be "weaker" than the soft soil's one, the main soil's fracture occurs in the soft soil with a curved pattern.

Keywords: Numerical analysis, soils fracture propagation, reverse faulting.
連絡先　〒153-8885　東京都目黒区駒場 4-6-1 生産技術研究所 Bw-206 小長井研究室　TEL 03-5452-6098

Let's introduce, because afterwards it will be useful, its linear approximation with a dip angle α*, in this case 50°, as shown in Fig. 2.

Over-all strain is a non-dimensional parameter defined as $\gamma_{rup} = \Delta_H/H$, which is the normalized bedrock displacement required to propagate the shear rupture zone to the ground surface, and its dependency on soil properties has been discussed in e.g. [1] and [4].

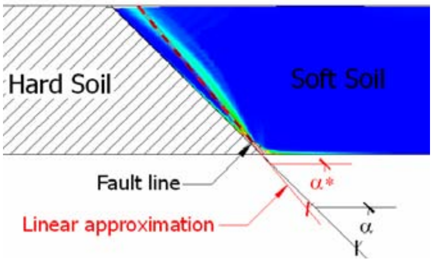

Fig.2 Localization in the soft of the main fracture after the bedrock displacement (Δ_F) and linear approximation of the curved rupture propagation with α*.

To estimate the over-all strain, γ_{rup}, with the numerical tool, we have used the necessary amount of Δ_F to cause a local inclination value of 1/200 of the model's surface; This corresponds to the soil inclination limit for avoiding damages on a reinforced concrete structures (Meyerhof, 1956).

4. Analytical model. A simple beam model for describing the rupture propagation has been introduced in [2]. A pair of elastic beams with the same length *L* and width *A* are compressed together through Winkler-type bi-linear springs (Jenkins element) as illustrated in Fig. 3. Each Jenkins element is a combination of a spring *k* and a slider ϕ arranged in series. The beams are confined together by the pressure *p*, which increases linearly with the increasing distance *x* from the top. The bottom ends of these beams are subjected to a pair of opposite axial displacements $\pm\Delta_F/2$. The solution of its governing equations, assuming that the ratio L/A is constant, compatibly to the previous introduced parameters, is:

$$\gamma_{rup} = \frac{\Delta_H}{H} \cong \frac{\sin\phi_S \cos\phi_S}{\left[1 - \sin\phi\cos\left(2\alpha - \pi/2 + \phi\right)\right]\cdot\sin\alpha}\,\frac{H\,\rho\,g}{E} \qquad \text{(eq.1)}$$

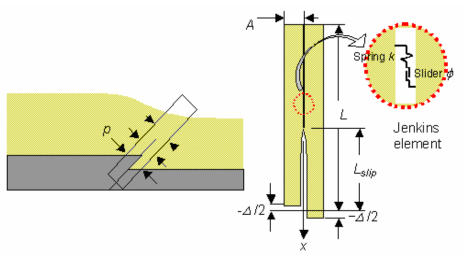

Fig.3 Paired beams for modeling fault rupturing

5. Comparison between solutions. The comparison between the numerical solution and the analytical solution under the common parameters show same trends: γ_{rup} increases for increasing ϕ, ρ, H and decreasing E.

Due to the fact that for the analytical solution, the direction of the fracture path has to follow necessary its initially assigned dip angle α; the numerical solution, according to [3], instead for low dip angles deviates from it's initial assigned dip angle: to compare the solutions it's necessary to consider the dip angle value of the linear approximation (α*) (see Fig. 4).

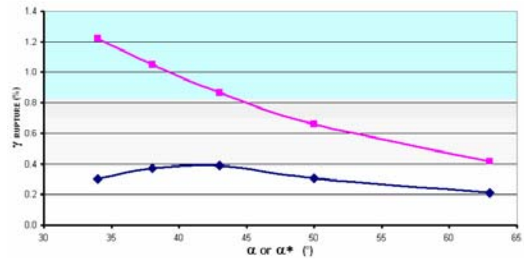

Fig.4. Numerical solution $\gamma_{rupture}$ vs. α* (lower curve) and Analytical solution $\gamma_{rupture}$ vs. α (upper curve).

6. Conclusions. We have used numerical and analytical tools for investigating the complex problems of reverse faulting through quaternary soils. The tools are compared by a common solution of over-all strain, γ_{rup}, and in particularly they show its behaviour when its constitutive parameters are varying and are able to produce their trends. Different tools are showing mostly same behaviours. The comparisons objective is not to obtain a rigorous solution but to offer a proper perspective on the key parameters that will govern the real fault rupturing. The validation of the numerical tool with the analytical solution can permit to extend the parametric study on the other not common parameters.

Reference

[1] BRAY J.D., SEED R.B. and SEED H.B., *"Earthquake fault rupture propagation through cohesive soil"*, Journ. Geotech. Eng., 120 (3), pp. 562-580, 1990.

[2] KONAGAI K., *"Simple beam model for describing rupture propagation"*. Unpublished document, Institute of Industrial Science, University of Tokyo, May 2004.

[3] COLE D.A., LADE P.V., *"Influence zones in alluvium over dip-slip faults"*, Journ. of Geotech. Eng., 110 (5), pp. 599-615, 1984.

[4] TANI K., UETA K. and ONIZUKA N., *"Scale effect of quaternary ground deformation observed in model tests of vertical fault"*, Proceedings of 29th Japan National Conference on Soil Mechanics and Foundation Engineering, pp.1359–1362, 1994 (in Japanese).